What's Weathering in Mine Waste? Mineralogic Evidence for Sources of Metals in Leachates

Sharon F. Diehl[1], Philip L. Hageman[2], Kathleen S. Smith[3], Koenig, A.E.[4], Fey, D.L.[5], and Lowers, H.A.[6]

[1-6] U.S. Geological Survey, Box 25046, Denver, CO 80225-0046; diehl@usgs.gov

Abstract

Microscale mineral-dissolution and precipitation reactions in mine-waste material provide insight into macroscopic weathering processes in waste piles and sources of metal concentrations in leachate solutions. Fluid movement and alteration processes at the microscopic scale are also important in the development of rock fabrics such as porosity that influence transport of materials through a mine-waste pile. Mine-waste piles are dynamic physical and chemical systems, as evidenced by partial to total dissolution of sulfide and other minerals, alteration rinds and etch pits on grains, secondary minerals that replace sulfide minerals, and precipitation and migration under low-temperature conditions of secondary evaporative minerals.

From the late 1800s through the early 1900s, gold and base-metal mining in the Leadville and Montezuma districts, Colorado, left extensive waste piles that contain Pb, Zn, Cu, and Fe sulfide minerals. Weathering of the sulfide minerals generates acid and releases metals at potentially toxic levels to receiving streams. Mine-waste materials from the Dinero, Lower Chatauqua, and Sts. John sites exhibit rock fabrics that indicate that weathering products─Fe oxyhydroxides, jarosite, and clays─have been transported in suspension through the waste piles and deposited in voids and as coatings on rock fragments.

The source of readily leachable metals in these mine-waste sites is revealed by microscale characterization of weathered, partially dissolved minerals. For example, mineralogic studies show that galena in the Lower Chatauqua and Sts. John waste is enriched in Ag relative to galena in Dinero waste. Qualitative and semiquantitative microanalysis of weathered, altered galena grains from all three sites show that the Ag-bearing galena is more susceptible to dissolution. It is not surprising, then, that solutions experimentally leached from Lower Chatauqua and Sts. John waste are higher in Pb (2,310 and 1,360 ppb, respectively) compared to leachates from the Dinero waste (31 ppb).

The mobility of most metals is increased under acidic conditions. Using the USGS Field Leach Test protocol, leachate derived from the Dinero waste has a pH of 3 and high concentrations of Al (443 ppb), Fe (441 ppb), and Zn (7970 ppb). Leachate from the Sts. John tailings has a pH of about 4 with high concentrations of Mn (1,520 ppb), Zn (2,240 ppb), and Pb (1,360 ppb). Leachate from the Lower Chatauqua waste has a circumneutral pH of 5, but in addition to the high Pb level already mentioned, it contains high levels of K (1.9 ppm), Mn (6,720 ppb), and Zn (1,550 ppb). The high concentrations of metals, despite the intermediate pH of the leachate, may be explained by acidic microenvironments that exist at the surfaces of sulfide minerals, where sulfur- and iron-oxidizing microbes may flourish. It is at the reactive mineral-oxygen-water interface where metals and acid are released and low-pH sulfate precipitates such as jarosite-beudantite form.

Introduction

Gold and base-metal mining in the late 1800's and early 1900's in the Leadville and Montezuma districts of Colorado left extensive waste piles, containing Pb-, Zn-, Cu-, and Fe-sulfides (Figs. 1, 2). Weathering of the sulfide minerals has generated acid mine drainage and released metals at toxic levels to surface waters and stream sediments, causing a negative impact on downstream aquatic biota (Bureau of Land Management, Colorado, 2003; Yang, 2006). The mining districts are located in mountainous terrain at elevations greater than 10,000 feet; therefore, mine-waste material is situated on steep slopes or in drainages subject to rapid stream flow. Due to steep topography, mining was conducted through horizontal adits (Ritter, 1908). Many of these adits such as at Dinero and Lower Chatauqua are open and drain into local watersheds (Walton-Day et al., 2005).

Understanding relationships between mineralogy, texture, microstructural features, and element distribution and residence in minerals is critical for accurate modeling of mineral weathering in waste-rock piles (Hammarstrom and Smith, 2002). Mine-waste piles have considerable void space that allows air and water infiltration, and hence, oxidation and weathering of rock fragments and minerals. Scanning electron microscope (SEM), electron microprobe (EPMA), and laser ablation inductively coupled plasma mass spectrometer (LA-MS-ICP) analysis of mine-waste samples from the Leadville and Montezuma districts have revealed mineralogic and microstructural controls on the mode of occurrence of minor and trace elements, the influence of trace metal content on weathering of sulfide minerals, and the release of metals into drainage systems. Dissolution textures in sulfide and silicate minerals in waste piles are direct evidence that weathering of these minerals is a primary source of elevated metal content and acidity in watersheds. Our objectives in characterizing the waste material were to: (1) identify the mineralogic source of the metals in solution, whether from the weathering of primary sulfide minerals, or the dissolution of secondary mineral precipitates, or both, and (2) relate the leachate results of the U.S. Geological Survey Field Leach Test (FLT) to minerals that exhibited dissolution textures (Hageman and Briggs, 2000; Diehl et al., 2005; U.S. Geological Survey, 2005). Metals in the USGS FLT leachates are an indication of reactive and soluble phases in the waste piles.

Geological Setting

The Leadville and Montezuma districts are located near timberline, at approximately 10,500 to 11,000 feet in elevation, in areas of Precambrian schist, gneiss, and granite (Lovering, 1935; Singewald, 1955) (Fig. 1). The schist and gneiss of the Rocky Mountain physiographic province may be correlated with the Early Proterozoic Swandyke Hornblende Gneiss and the Idaho Springs Formation of the Front Range of Colorado, and the granite may be correlated with the Middle Proterozoic Silver Plume granite (Singewald, 1955). Unaltered host rock is resistant to weathering and forms a steep topography. During the Late Cretaceous Laramide Orogeny, the region was highly deformed by orthogonal fault sets and the emplacement of veins.

The Dinero and Lower Chatauqua waste piles are composed of rock fragments that range from boulder-size to very fine-grained matrix material and are a composite of different rock types, gneiss, granite, and porphyry (Fig. 2). Surficial weathering differentiates areas of brown iron-oxide alteration, grayish zones with sulfidic material, black manganoan streaks, and white areas of soluble efflorescent minerals (Fig. 2). Rock fragments of veined material host manganoan carbonate with galena, pyrite, chalcopyrite, and Ag-sulfide minerals. Barite is a common accessory mineral. Feldspar was highly altered during ore mineralization and is commonly partially to totally altered to fine-grained potassic sericitic clays.

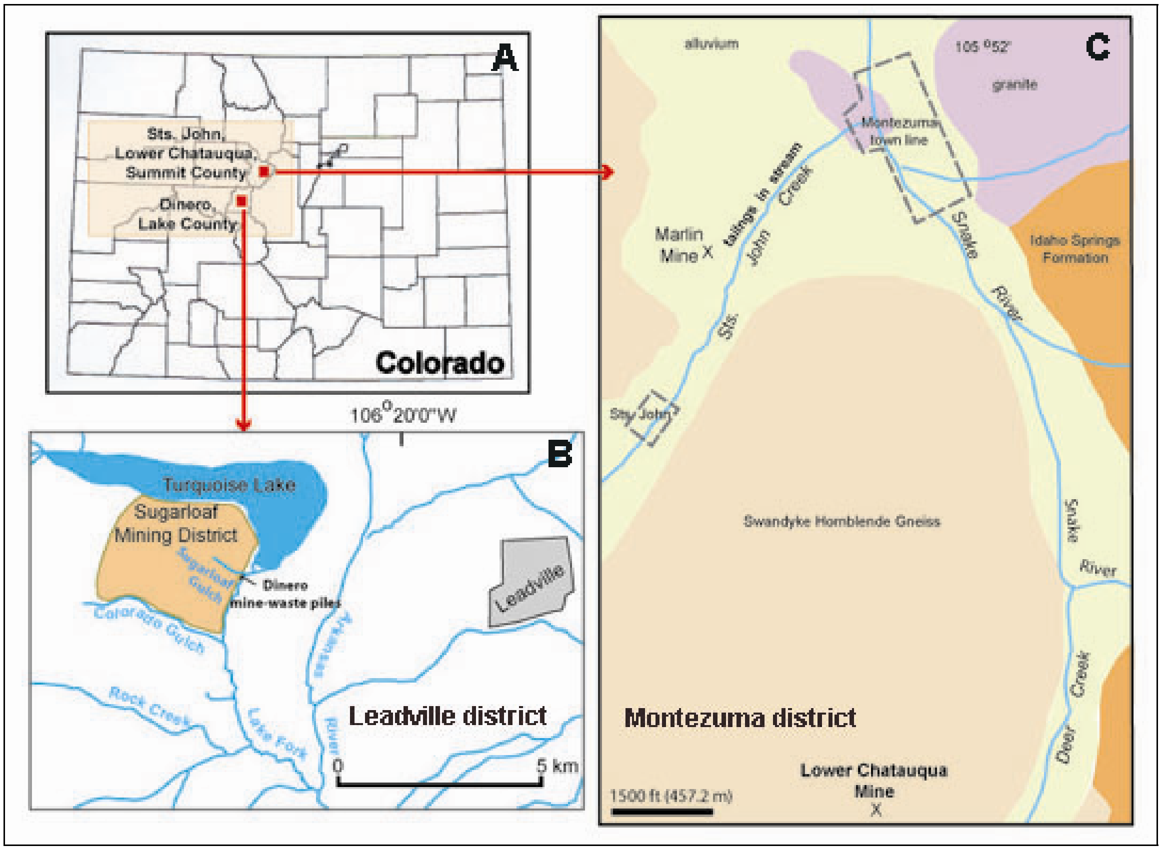

Figure 1. Location maps of mine-waste sites, drainage systems, and general geology. A. Map of Colorado showing locations of Summit and Lake Counties. B. Location map of the Dinero waste pile in the Sugarloaf Mining District, Leadville, Colorado. C. Location map of the Lower Chatauqua mine waste site, and Sts. John wetland.

Stream sediments in Sts. John Creek largely consist of well-sorted, sand-size mine tailings of sulfide minerals, Fe-Mg minerals, micas, barite, and quartz grains. The tailings are composed of various types of ore from around the region that were processed at the Sts. John mill and town site (Fig. 1C).

Methods

USGS Field Leach Test

The USGS FLT protocol was followed to leach composite mine-waste samples from the Dinero and Lower Chatauqua mine-waste piles and from tailings in the wetland downstream from the Sts. John mill site (Hageman and Briggs, 2000; Smith et al., 2000; Smith et al., 2002; U.S. Geological Survey, 2005). Complete details of the non-grid sampling technique and the leaching procedure are fully described in USGS Fact Sheet 2005-3100 (U.S. Geological Survey, 2005). Fifty grams of a representative mine-waste sample that includes all lithologies, sieved to a < 2 mm size fraction is combined with 1.0 L of deionized water. The mixture is shaken, allowed to settle, and filtered. The filtrate was analyzed in the lab for 44 elements, using inductively coupled plasma-mass spectrometry (ICP-MS); thirteen elements are reported here (Table 1; Briggs, 2002; Lamothe et al., 2002).

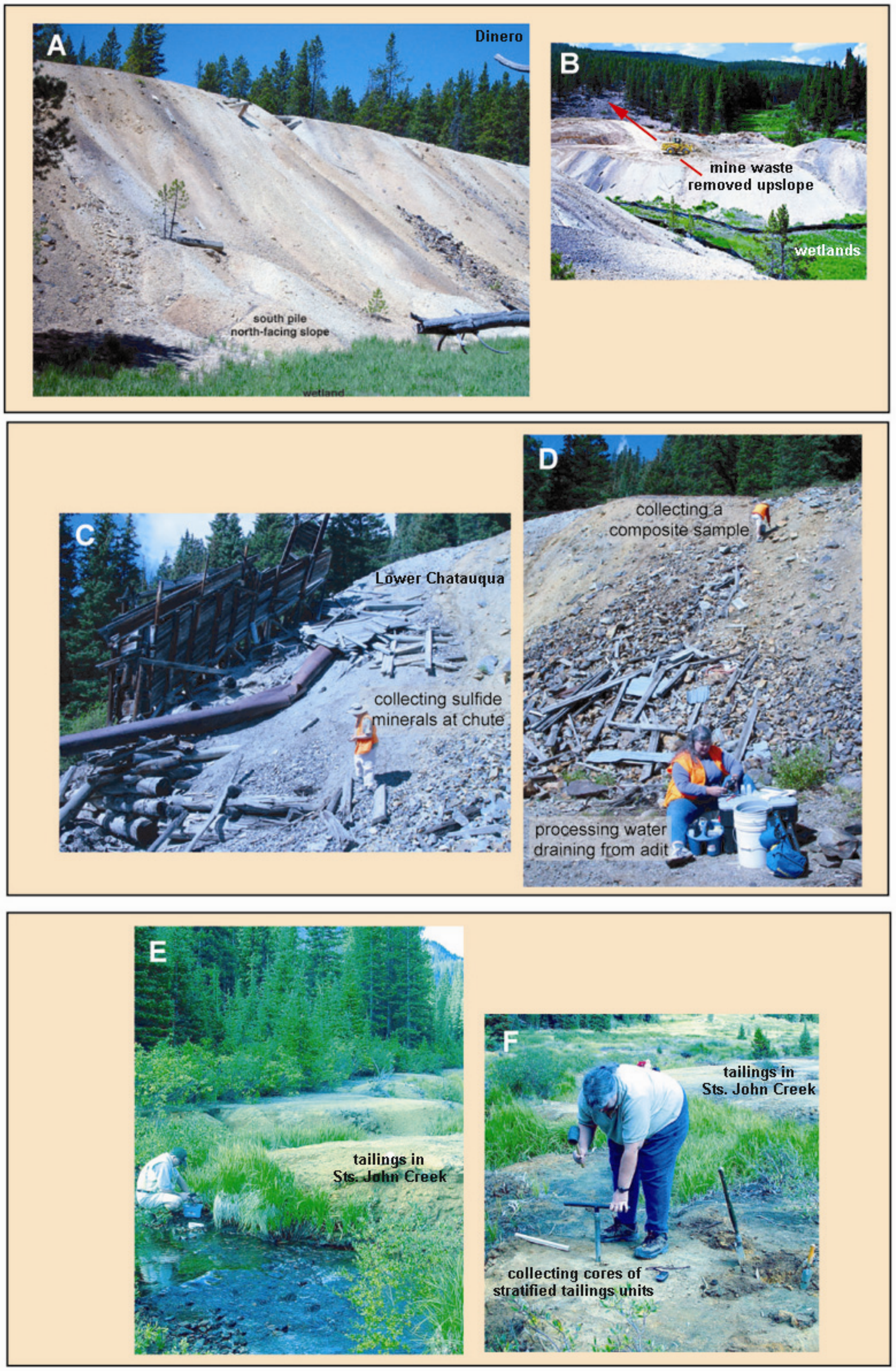

Figure 2. **A-B**. Dinero waste piles, Leadville District, Colorado, before remediation efforts. **C-D**. Lower Chatauqua mine-waste pile, Montezuma district, Colorado. **E-F**. Tailings in Sts. John Creek, Montezuma district, Colorado.

Filtered (0.45 μm), acidified samples of efflorescent salts from the Dinero waste site were analyzed by inductively coupled plasma-atomic emission spectroscopy (ICP-AES). Efflorescent salt samples were also analyzed by X-ray diffraction (XRD). XRD patterns were collected on a Scintag X-1 theta-theta diffractometer.

Microscopic and Microanalytical Methods

In addition to geochemical analysis, selected samples were examined in transmitted and reflected light microscopy. Both polished and whole mine-waste samples were examined with a JOEL 5800LV scanning electron microscope (SEM), equipped with an Oxford ISIS energy-dispersive X-ray (EDS) detector to determine basic mineralogy, analyze structural and textural features, and for qualitative to semi-quantitative analysis of trace- and minor-element content, and distribution in minerals. Digital element maps, showing the spatial distribution of S, Fe, Zn, Pb, Co, Ni, As and other associated elements, were generated on a JEOL JXA-8900 electron probe microanalyzer (EMPA).

Polished samples of sulfide-bearing rock fragments were analyzed using a laser ablation inductively coupled plasma mass spectrometer (LA-ICP-MS, Ridley and Lichte, 1998; Ridley, 2000). Quantitative trace element data was gathered using a Perkin-Elmer Sciex Elan 6000 quadrupole mass spectrometer attached to a CETAC LSX500 laser system. A 50-micron-beam size was used to analyze for trace elements in pyrite. USGS sulfide standard MASS-1 (formerly PS-1, Wilson et al., 2002) was used as a calibration standard.

Each instrument, SEM, EMPA, and LA-ICP-MS, used for minor- and trace-element analyses, has its benefits and limitations. SEM and EMPA have excellent spatial resolution (better than a few microns). LA-ICP-MS has better sensitivity for a wider range of trace elements. If element content is below the limit of detection to x-ray map with the SEM or EMPA (~<500-1000 ppm), the LA-ICP-MS can determine element concentration to less than 1 ppm. The choice of methods used depends on what questions need to be addressed, e.g., is the trace-element bulk concentration or residence site more important in a particular study?

Results and Discussion

Leachate Chemistry

Table 1. Results of the U.S. Geological Survey Field Leach T (20:1 water/rock ratio); element concentration reported in ppb = parts per billion; bdl = below detection limit.

Sample Locality;	Spc	pH	Al	As	Ba	Cd	Co	Cu	Fe	K	Mn	Ni	Pb	Ti	Zn
Dinero	845	3.30	443	2	91	50	1.64	49	441	880	1250	8	31	6.6	7970
Lower Chatauqua	197	5.03	3	bdl	116	9	2.36	22	bdl	1900	6720	13	2310	1.4	1550
Sts. John	170	3.55	52	1	130	9	1.58	30	bdl	630	1520	3	1360	0.5	2240

The reactivity and mobility of most metals is increased at low pH. Therefore, high metal concentrations of Al, Fe, and Zn from the Dinero site are predictable because leachate from a composite mine-waste sample recorded a pH of 3.3 (Table 1). However, the high Pb, K, and Mn from the Lower Chatauqua site, where the leachate pH is 5, require explanation (Table 1). Dissolution pits and secondary mineral precipitates on the surfaces of sulfide minerals suggest that they are acidic microenvironments where sulfide- or iron-oxidizing microbes can flourish and enhance dissolution.

All mine-waste and tailings sampling sites contained galena (PbS) and sphalerite [(Zn,Fe)S]. However, Zn occurs in greater concentration in the leachate from the Dinero site, and Pb occurs in greater concentration in leachates from the Lower Chatauqua and Sts. John waste sites (Table 1).

Weathering Products

Weathering induces fragmentation of the rock particles. Rock fragments break down along grain boundaries and transgranular fractures that are lined with iron oxides and other secondary minerals. Freezing and thawing at high elevation may be a major contributor to the breakdown of the larger boulders.

Dissolution of Minerals. At all the waste sites, minerals such as pyrite (FeS_2), chalcopyrite ($CuFeS_2$), sphalerite, galena, and ilmenite ($FeTiO_3$) show partial to total dissolution (Figs. 3A, 3B). The existence of precursor mineral grains is commonly inferred on the basis of iron-oxide boxwork skeletal remnants and euhedral outlines of voids (Figs. 3A, 3B). Trace element-rich minerals that undergo dissolution are sources of elevated metal concentration in drainages. For example, sulfide minerals such as pyrite commonly host arsenic; galena frequently contains Ag; sphalerite has Fe and Cd; and jarosite commonly contains Pb, Ag, Cu, or Zn constituents. Trace-element content may increase the solubility of a mineral by substitution of elements, such as As for S in pyrite, Ag for Pb in galena, or Cd for Zn in sphalerite (Savage et al., 2000; Diehl et al., 2003). Element substitution changes physical properties of the minerals and may distort the lattice structures (Lehner and Savage, 2004), increasing the susceptibility of the mineral to dissolution. For example, Cd and Zn are elements of concern in waters draining from the Dinero waste site. A comparison of element distribution maps of sphalerite between the Dinero and Sts. Johns waste shows that Cd-rich sphalerite in Dinero waste is deeply etched and partially dissolved, whereas sphalerite at the Sts. John site that hosts minor amounts of Cd (Figs. 3C, 3D) commonly shows minor dissolution features.

Table 2. Laser ablation ICP-MS results of pyrite analyses from the three mine-waste sites.

Location	Number of Spot Analyses	Ag (ppm)	Cd (ppm)	Co (ppm)	Cu (ppm)	Ni (ppm)	Pb (ppm)
Dinero	N = 19	361	27	7	369	20	2649
Sts. John	N = 22	95	2.6	20	554	97	331
Lower Chatauqua	N = 6	71	19	158	169	120	8368

LA-ICP-MS analyses of pyrite from the three mine-waste sites demonstrate the high concentration of trace metals that can be hosted in sulfide minerals (Table 2). The high Co, Ni, and Pb numbers in the

Lower Chatauqua pyrite are significant. Biologists have conducted a study in streams below mine-waste sites in the Montezuma district, linking metal content in water and aquatic biota, to metal content in organs of nestlings of swallows. The highest metal concentrations in benthic invertebrates in the district occur in Deer Creek below the Lower Chatauqua site (Fig. 1) (Yang, 2006). During the period of the study, no swallows nested at the locality along Deer Creek where the metal content in aquatic food sources was the highest (Yang, 2006).

Microbial Activity. Scanning electron photomicrographs of sulfide minerals collected from the surface of the Dinero and Lower Chatauqua mine-waste piles show euhedral etch pits and other dissolution textures. These textures are consistent with laboratory studies of the formation of etch pits and dissolution embayments on mineral surfaces by sulfur-oxidizing microorganisms (Edwards et al., 2000) (Figs. 3E, 3F). As dissolution of the mineral surface proceeds, etch pits enlarge and combine. Secondary sulfate minerals such as anglesite fill etch pits in galena and eventually coalesce into layers (Fig. 3F).

Formation of Secondary Minerals. Potassium jarosite is the most common jarosite phase at these waste sites, but Na-, Pb- and Ag-bearing jarosite, and beudantite [$PbFe_3(AsO_4)(SO_4)(OH)_6$] are also present (Figs. 3G, 3H). Jarosite is commonly less than 2 µm in diameter. Grain-size clusters of submicron K-jarosite and beudantite suggest total replacement of sulfide minerals by secondary sulfate pseudomorphs.

Low-pH fluids can attack minerals such as biotite and muscovite, releasing K^+, which is then available to form K-jarosite. Figure 4A shows a mica grain in early stages of weathering, the darker areas at the exfoliated edges of the mica show the loss of K and heavy elements such as Fe and Ti. Potassium and Pb-jarosite commonly occur between cleavage planes in altered exfoliated muscovite (Fig. 4B).

Galena (PbS), commonly exhibits alteration rims of anglesite ($PbSO_4$) (Fig. 4C). The fine-grained porous anglesite alteration rinds show partial to total dissolution, suggesting that the weathering of the galena to anglesite, and dissolution of anglesite, is a primary source for aqueous Pb^{2+}. Figure 4D shows dissolution embayments at the interface between the galena grain and the fine-grained porous anglesite. The penetration of the dull-gray anglesite alteration product into the brighter light-gray galena grain (Fig. 4D) demonstrates that this interface is an important reaction/alteration zone where metals enter into solution. This reactive interface also demonstrates that the rind of anglesite does not function as a protective barrier against fluid infiltration because the anglesite is very fine grained (reactive) and has a porous texture.

Soluble Salts. Water-soluble salts, formed by evaporation of acidic, metal-bearing solutions, were collected from a seep on the remediated south Dinero waste pile and from the edge of a remediation pond below the open Dinero adit. These white, metal-sulfate minerals form crusts on waste material and vegetation. X-ray diffraction analysis shows the presence of starkeyite ($MgSO_4 \cdot 4H_2O$), gunningite [$(Zn, Mn) SO_4 \cdot H_2O$], and gypsum ($CaSO_4 \cdot 2H_2O$). ICP-AES analysis shows that metals such as Cd, Co, and Ni are stored in the soluble salts (Table 3). Because these efflorescent salts dissolve rapidly, they are a source of acid and metals during every precipitation event.

An advantage of examining the secondary evaporative minerals with the SEM is that 3-dimensional samples can be mounted and analyzed. This direct analytical method allows us to determine the degree of crystallinity of the evaporative minerals, the sequence of precipitation of minerals, and preferred metal associations (Fig. 4E). A major element distribution map of a soluble salt sample from Dinero waste shows that Mg-rich coarse-grained crystals precipitate first, followed by Mn-rich fine-grained crystals (Fig. 4E). Features of the Zn map are subtle, but it appears that Zn preferentially precipitates early with Mg (Fig. 4E). Gypsum was commonly the last mineral to precipitate, in fibrous, radiating masses, coating both the Mg- and Mn-bearing minerals.

Table 3. Selected element concentration results of ICP-AES analysis of efflorescent soluble salts, Dinero waste site. Data are in parts per million (ppm) except where noted.

Sample Locality (Dinero)	Al (%)	Cd	Co	Cu	Fe (%)	K (%)	Mn (%)	Ni	Zn	SO_4
Seep in waste repository	0.065	350	340	12	0.009	0.448	5.8	400	238000	570
Remediation Pond	0.110	61	290	27	0.024	0.165	1.7	340	233000	450

Infiltration of Fluids and Transport of Material

Weathering and vertical transport of material within the Dinero and Lower Chatauqua waste piles was evidenced by clay coatings and clay drapes on mineral grains and rock fragments, and by geopetal fabrics (features that demonstrate vertical orientation), such as fine-grained minerals that partially fill dissolution voids, or amorphous material that has settled out of suspension into distinct chemical layers (Fig. 4F). Matrix material is largely composed of jarosite [$KFe^{3+}_3 (SO_4)_2 (OH)_6$], potassic clays, amorphous iron oxides and silica; rock fragments are commonly coated by amorphous iron-oxide material (Fig. 3A).

Amorphous Fe-Sulfate, Fe-Oxide, and Fe-Oxyhydroxide Material. Scanning electron photomicrographs show amorphous iron-sulfate and iron-oxyhydroxide material coating rock fragments and filling voids in weathered mine waste as microlaminated sedimentary deposits (Fig. 4F). The development of microlaminated material in the voids of mine-waste piles is similar to illuvial accumulations of clays and other materials in voids and fractures in soils. The microlaminated textures are important indicators that this amorphous alteration material was flushed through the mine waste during wetting events and deposited out of suspension during periods of dryness. The microlaminated void-fill material exhibits sedimentary features, such as cross beds and soft sediment slump structures (Fig. 4F). The light and dark microlaminations indicate fluctuations in metal content during deposition. Again, this is evidence that iron-bearing solutions–that were generated from the weathering of pyrite–precipitated in voids after primary weathering of sulfides occurred.

Amorphous Mn-Oxyhydroxide Material. Amorphous Mn oxyhydroxide is a common aqueous precipitate in the Sts. John tailings and occurs as coatings on stream sediment grains, as a cement around fresh-water diatoms and shell material, and as replacement of cellular plant material (Fig. 4G). Manganese oxides and oxyhydroxides may be produced by bacterial action (Robbins et al., 1999). Mn oxyhydroxides are capable of sorbing metals (Fuller et al., 2005), and these Sts. John Mn-precipitates host Ba, Cu, Pb and other trace metals (Fig. 4G).

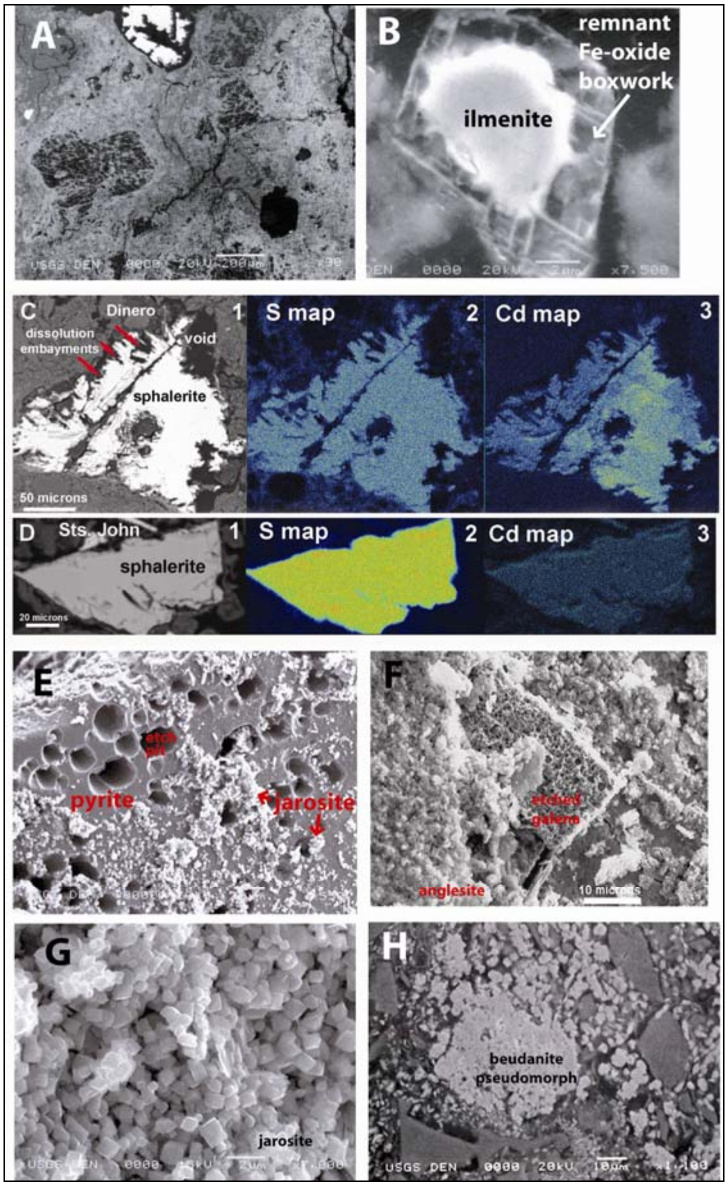

Figure 3. **A.** Sulfide and oxide minerals undergo dissolution, commonly leaving only boxwork skeletons, masking their original mineralogy (Dinero site). Backscatter electron image (BSE) of mine-waste thin section sample, showing euhedral voids left by the total dissolution of grains, Fe-oxide skeletal remnants of grains, and partial dissolution of a pyrite grain. **3B**. BSE image of partially dissolved grain of ilmenite, FeTiO$_2$. Remnant alteration rims around grains have been described as "atoll-type" textures by Jambor (2003). **3C-D**. **C1.** BSE image of an etched, partially dissolved sphalerite grain from the Dinero waste pile. **C2.** EPMA distribution map of Zn, which outlines the sphalerite grain. Yellow colors = higher concentrations; blue colors = lower concentrations of an element. **C3.** EPMA distribution map of Cd in sphalerite grain. **D1.** BSE of sphalerite from Sts. John tailings. **D2.** Zn element map. **D3.** Cd element map. In comparison to Dinero sphalerite (A3), sphalerite from the Sts. John waste lacks high concentrations of Cd. **3E**. SEI image of etched, altered pyrite grain from the surface of Lower Chatauqua mine-waste pile. Jarosite is associated with euhedral etch pits, which may have formed as a result of activity by sulfur-oxidizing microbes. **3F**. Secondary electron image (SEI) of an altered galena grain from Lower Chatauqua mine-waste pile. Bulbous clusters of PbSO$_4$ coalesce to form alteration layers of anglesite, coating galena grain. Etch pits develop as anglesite precipitates. **3G.** Dinero mine waste. SEI image of micron to submicron size jarosite minerals in matrix material between rock fragments. **3H.** SEI image of grain-size area of submicron beudantite crystals, suggesting total replacement of the original mineral.

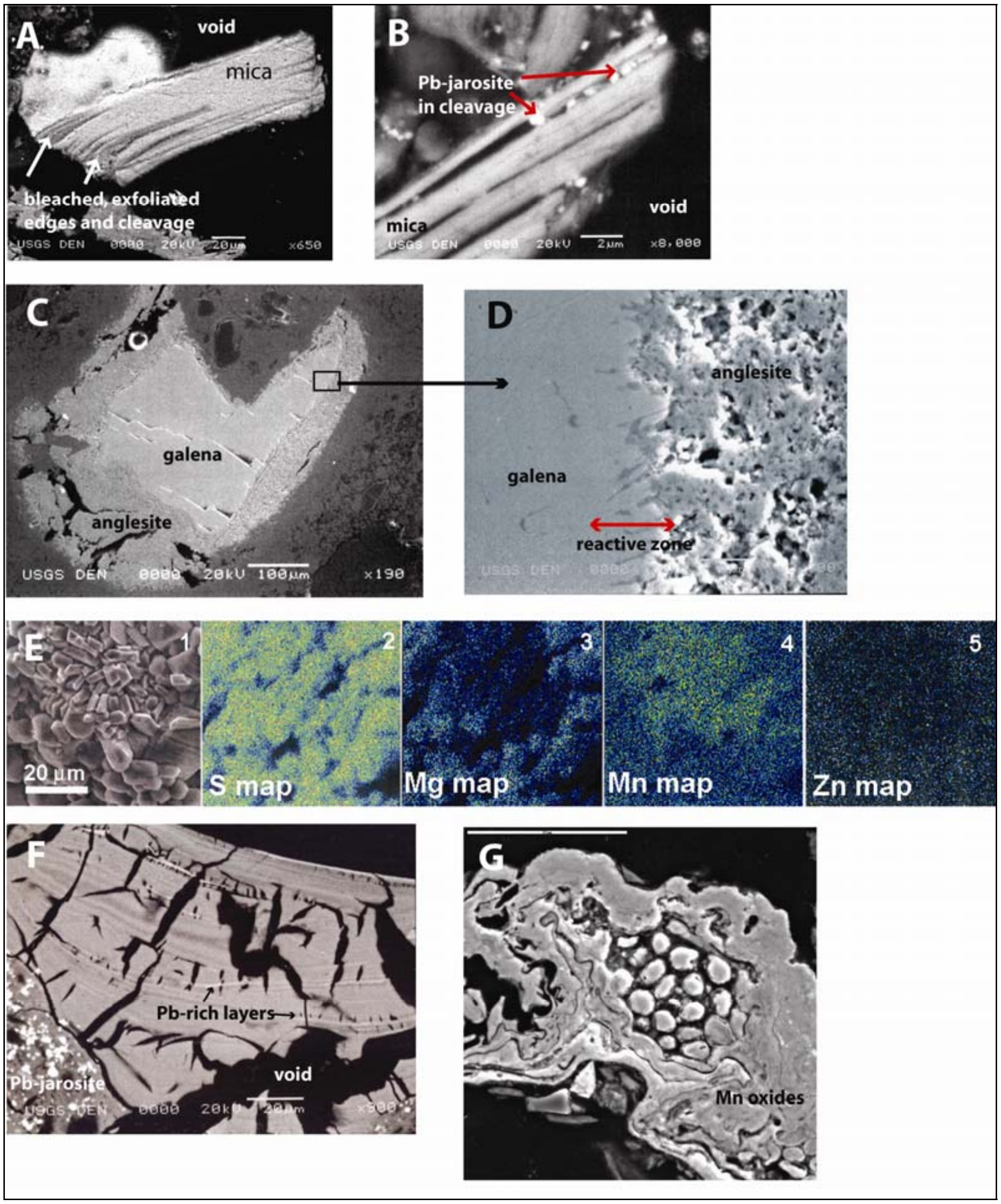

Figure 4. **4A**. BEI image showing early stage of weathering of mica grain. Duller areas along cleavage indicate leaching of K, Fe, and Ti. **4B**. Pb-jarosite between cleavage planes of altered muscovite. **4C**. Dinero mine waste. SEI image of galena with an alteration rim of anglesite ($PbSO_4$). Black square is area shown in 4D. **4D**. Close-up SEI image of the altered, etched interface between galena and anglesite. Note the penetration of anglesite into the galena grain. **4E**. **1**. SEI image of 3-dimensional sample of soluble salts at surface of seep, Dinero waste. **2**. Sulfur (S) element distribution map of soluble salts, showing that both the fine- and coarse-grained minerals are sulfates. **3**. Mg element map shows that the coarse-grained crystals are a Mg-rich sulfate. **4**. Mn element distribution map, showing that the euhedral fine grained crystals are a Mn-rich sulfate. **5**. Zn element distribution map. Although subtle, Zn preferentially precipitated with the Mg sulfate. **4F**. BSE image of amorphous Fe-oxyhydroxides and sulfates filling a void, Lower Chatauqua. Microlaminations exhibit a cross bedded sedimentary, geopetal texture in the void. Bright grains in matrix are Pb-jarosite. BSE image shows several generations of void fill sediments, recorded by the difference in brightness (i.e. chemistry) in each microlayer. Shrinkage cracks and partial dissolution of this amorphous material demonstrate the instability of this cement between rock fragments. **4G**. Mn-oxide/oxyhydroxide replacement of cellular organic material.

Summary

Researchers are utilizing a number of analytical techniques to address issues of metal contamination in receiving streams and to identify sources of elements, their mode of occurrence, i.e., where elements reside in minerals or structures, and their concentration. This study has made extensive use of direct microanalytical techniques such as the SEM and EPMA in conjunction with chemical analyses to study mineral sources of metal contamination in drainages below abandoned mine sites. Understanding the mode of occurrence of major, minor, and trace elements and the relationship between textural and chemical properties of waste rock provides insight into the sources and pathways of metal contamination.

This study shows the relation between the weathering of components of a waste-rock pile and what is observed in leachate solutions:

1. Partial to totally dissolved minerals are evidence that solutions within the waste-rock pile are responsible for the dissolution of primary sulfide, oxide, and silicate minerals. Weathering of the mine-waste minerals, especially through the processes of dissolution, increases permeability in the mine waste pile, and therefore increases fluid and oxygen access, which in turn can accelerate the rate of dissolution at the mineral-water interface.
2. Secondary mineral cements, that form in the waste pile during dry periods and readily dissolve during wet periods, are evidence for the penetration of fluids deep into the pile.
3. The formation of anglesite and efflorescent salts are evidence that the primary sulfides and silicates weather into sulfates and oxides that are much more soluble than the original host mineral.

Acknowledgments

This work was funded by the USGS Mineral Resources Program. The Colorado Division of Minerals and Geology and the Bureau of Land Management Lake Fork Watershed Group allowed us access to the mine-waste piles and permitted sampling at the Dinero site. Steve Sutley, USGS, Denver, analyzed X-ray diffraction patterns of the efflorescent salts from the Dinero waste site. (Note: mention of trade names or commercial products is for descriptive purposes only and does not imply endorsement by the U.S. Government.)

References

Bureau of Land Management (BLM), Colorado, 2003. Lake County Watershed Water Quality Assessment, Point and Non-Point Source Pollution Inventory and Evaluation. Request from BLM Abandoned Mine Lands Cleanup program: http://www.blm.gov.aml/.

Briggs, P.H., 2002. The determination of twenty-even elements in aqueous samples by inductively coupled plasma-atomic emission spectrometry. In Taggert, J.E., Jr., ed., Analytical Methods for Chemical Analysis of Geologic and Other Materials: U.S. Geological Survey Open-File Report 02-223, p. F1-F11. (Available online at: http://pubs.usgs.gov/of/2002/ofr-02-0223/)

Diehl, S.F., Smith, K.S., Desborough, G.A., Goldhaber, M.B., and Fey, D.L., 2003. Trace-metal sources and their release from mine wastes: Examples from humidity cell tests of hard-rock mine waste and from Warrior Basin coal: National Meeting of the American Society of Mining and Reclamation and 9th Billings Land Reclamation Symposium, Billings, MT, June 3-6, CD ROM.

Diehl, S.F., Hageman, P.L., and Smith, K.S., 2005. Sources of acid and metals from the weathering of the Dinero waste pile, Lake Fork Watershed, Leadville, Colorado. In Barnhisel, R.I., ed., Proceedings, 22nd National Conference, American Society of Mining and Reclamation, Breckenridge, CO, June 19-23, p. 268-282.

Edwards, K.J., Bond, P.L., and Banfield, J.F., 2000. Characteristics of attachment and growth of *Thiobacillus caldus* on sulphide minerals: a chemotactic response to sulphur minerals? Environmental Microbiology, v. 2, p. 324-332.

Fuller, C., Bargar, J.R., and Webb, S.M., 2005. Processes of Zn attenuation by biogenic manganese oxides forming in the hyporheic zone of Pinal Creek, Arizona, USA: Geological Society of America Annual Meeting, Abstracts with Programs, v. 37, no. 7, p. 323.

Hageman, P.L., and Briggs, P.H., 2000. A simple field leach test for rapid screening and qualitative characterization of mine waste dump material on abandoned mine lands. In Proceedings from the Fifth International Conference on Acid Rock Drainage (ICARD2000), Denver, Colorado, May 21-24: Society for Mining, Metallurgy, and Exploration, Inc., v. II, p. 1463-1475.

Hammarstrom, J.M., and Smith, K.S., 2002, Geochemical and mineralogic characterization of solids and their effects on waters in metal-mining environments in Seal, R.R., II, and Foley, N.K., eds., Progress on Geoenvironmental Models for Selected Mineral Deposit Types, Chap. B: U.S. Geological Survey Open-File Report 2002-195, p. 8-47.

Jambor, J.L., 2003. Mine-waste mineralogy and mineralogical perspectives of acid-base accounting. In Jambor, J.L., Blowes, D.W., and Ritchie, A.I.M., eds., Environmental Aspects of Mine Wastes: Mineralogical Association of Canada, Short Course Series, v. 31, chap. 6, p. 117-145.

Lamothe, P.J., Meier, A.L., and Wilson, S.A., 2002. The determination of forty-four elements in aqueous samples by inductively coupled plasma-mass spectrometry. In Taggart, J.E., Jr., ed., Analytical Methods for Chemical Analysis of Geologic and Other Materials: U.S. Geological Survey Open-File Report 02-223, p. H1-H11. (Available online at: http://pubs.usgs.gov/of/2002/ofr-02-0223/).

Lehner, S.W., and Savage, K.S., 2004. Synthesis and characterization of large Co, Ni, and As doped pyrite crystals produced by chemical vapor transport: Geological Society of America, Abstract with Programs, v. 36, no. 2, p. 82.

Lovering, T.S., 1935. Geology and ore deposits of the Montezuma Quadrangle, Colorado: U.S. Geological Survey Professional Paper 178, 119 p.

Ridley, W.I., 2000, Instruction manual for "Quantlaser"; a batch process macro for reduction of quantitative laser ablation data: U.S. Geological Survey Open-File Report 00-0311, 42 p.

Ridley, W.I., and Lichte, F.E., 1998, Major, trace and ultratrace element analysis by laser ablation ICP-MS *in* Shanks, W.C., McKibben, M.A., and Ridley, W.I., eds., Reviews in Economic Geology, v. 7, , p. 199-215.

Ritter, E.A., 1908. The Montezuma mining district, Colorado, revival of a lead-silver-zinc camp on an extension of the Georgetown and Silver Plume Mineral Belt: The Engineering and Mining Journal, v. 85, p. 241-244.

Robbins, E. I., Brant, D. L., and Ziemkiewicz, P. F. 1999. Microbial, algal, and fungal strategies for manganese oxidation at a Shade Township coal mine, Somerset County, Pennsylvania. In Bengson, S. A., and Bland, D. M., eds., Proc. 16th Annual National Meeting. ASMR, Mining and Reclamation. for the Next Millennium, Vol. 2. Aug. 13-19, 1999, Scottsdale, AZ, p. 634-640.

Savage, K.S., Tingle, T.N., O'Day, P.A., Waychunas, G.A., and Bird, D.K., 2000. Arsenic speciation in pyrite and secondary weathering phases, Mother Lode Gold District, Tuolumne County, California: Applied Geochemistry, v. 15, p. 1219-1244.

Singewald, Q.D., 1955. Sugar Loaf and Saint Kevin mining districts, Lake County, Colorado: U.S. Geological Survey Bulletin B 1027-E, p. 251-299.

Smith, K.S., Campbell, D.L., Desborough, G.A., Hageman, P.L., Leinz, R.W., Stanton, M.R., Sutley, S.J., Swayze, G.A., and Yager, D.B., 2002. Toolkit for the rapid screening and characterization of waste piles on abandoned mine lands. In Seal, R.R., II and Foley, N.K., eds., Progress on Geoenvironmental Models for Selected Mineral Deposit Types, chap. C: U.S. Geological Survey Open-File Report 02-195, p. 55-64.

Smith, K.S., Ramsey, C.A., and Hageman, P.L., 2000. Sampling strategy for rapid screening of mine-waste dumps on abandoned mine lands. In Proceedings of the Fifth International Conference on Acid Rock Drainage, Denver, CO, May 21-24, 2000: Society for Mining, Metallurgy, and Exploration, Inc., v. II, p. 1453-1461. (Available online at: http://crustal.usgs.gov/projects/minewaste/pdfs/kathy.pdf).

U.S. Geological Survey, 2005. A simple field leach test to assess potential leaching of soluble constituents from mine wastes, soils, and other geologic materials: U.S. Geological Survey Fact Sheet 2005-3100, 4 p. (Available online at http://pubs.usgs.gov/fs/2005/3100/)

Walton-Day, K., Flynn, J.L., Kimball, B.A., and Runkel, R.L., 2005. Mass loading of selected major and trace elements in Lake Fork Creek near Leadville, Colorado, September-October 2001: U.S. Geological Survey Scientific Investigations Report 2005-5151, 46 p. (Only available online at http://pubs.usgs.gov/sir/2005/5151/)

Wilson, S.A., Ridley, W.I., and Koenig, A.E., 2002, Development of sulfide calibration standards for the laser ablation inductively-coupled plasma mass spectrometry technique: Journal of Analytical Atomic Spectrometry, v. 17, p. 405-409.

Yang, Chi, 2006, Effects of acid mine drainage on nesting tree swallows: Master of Science thesis; University of Colorado, Boulder, CO, 94 pages.